Journal of Industrial and Engineering Chemistry 58 (2018) 266–277

Contents lists available at ScienceDirect

Journal of Industrial and Engineering Chemistry

journal homepage: www.elsevier.com/locate/jiec

Improving nanoparticle dispersions of pigment and its application to a color filter: New phthalocyanine derivatives as synergist

Jin Woong Namgoong[a], Sei-Won Chung[a], Hyeyoun Jang[a], Young Hoon Kim[b], Moo Sun Kwak[b], Jae Pil Kim[a,*]

[a] Department of Materials Science and Engineering, Seoul National University, Seoul 151-744, Republic of Korea
[b] Color Team, LG Display Co., Ltd., Paju-si, Gyeonggi-do 413-779, Republic of Korea

ARTICLE INFO

Article history:
Received 30 June 2017
Received in revised form 28 August 2017
Accepted 14 September 2017
Available online 23 September 2017

Keywords:
Pigment green 7
Nanoparticle
Pigment dispersion
Color filter
Phthalocyanines

ABSTRACT

Four synergists were synthesized to enhance pigment nanoparticles dispersion and the contrast ratio. The interaction between the synergist and the dispersant was confirmed by infra-red (IR) spectrometry. We demonstrate that the hydrogen bonds forming between the synergist and the dispersant act as a key factor. To analyze the dispersion properties, dynamic light scattering (DLS), and electron microscopic analysis was examined. The spectral and color characteristics was also measured by UV–vis spectrometry and colorimetry, and the contrast ratio of color filters was evaluated. This study confirms that the prepared synergist can increase the contrast ratio of green color filter.
© 2017 The Korean Society of Industrial and Engineering Chemistry. Published by Elsevier B.V. All rights reserved.

Introduction

In display devices using a backlight unit such as an LCD, especially, the particle size of the pigments affects not only chromatic properties such as brightness and color but also contrast ratio related to light scattering [1]. The large pigment particles in the color filter scatter the transmitted light. The polarization of the light is changed and becomes uncontrollable, resulting in a transmission of additional light and a decrease in the contrast ratio. Light scattering is related to the particle size, ratio of the refractive indices between the particle and surrounding medium, and particle shape. Among these factors, the particle size exerts a profound influence on the scattering of incident light [2]. Theoretically, larger particles cause more scattering than smaller particles, provided that the refractive index of the particles is the same [3].

For this reason, the solvent-based wet dispersion method with polymer dispersant is used to obtain fine particles, incorporated into an LCD color filter. To obtain a well-dispersed system, preventing the coagulation of the colloidal pigment is very important. This stabilization mainly occurs *via* electrostatic and steric stabilization. However, the former is induced in highly polar systems such as aqueous inks, while the latter is the primary factor in solvent-based systems [4]. Therefore, additives like a polymeric surfactant and synergists are added to obtain stabilized particles in a non-polar solvent, and these additives play a crucial role in producing fine particles. In the wet-dispersion process, the ground pigment powder is stabilized by a dispersing agent. The dispersing agent is adhered to the surface of the pigments after the wetting and grinding stage, and this adsorption of the dispersing agent leads to repulsion between the particles, thereby preventing the flocculation of the particles. The interaction between the dispersant and pigment particles could be induced by different types of force (*e.g.*, ionic, hydrogen-bonding, and electrostatic) [4].

However, in some organic pigments such as phthalocyanine and dioxazine derivatives, the pigment molecules are not responsive to any of the dispersants, owing to their large planar structures. Thus, dispersions of these pigments easily flocculate after grinding. This issue could be resolved by enhancing the interaction between the pigment and dispersant. The synergist can play this role by adsorbing on the pigment surface and then anchoring the dispersant. When the pigments are dispersed by using only the dispersant without a synergist, the dispersion performance including particle size is inferior, and the stability is also considerably reduced. In contrast, when synergists are introduced, the particle size and dispersion stability can then be improved, resulting in better chromatic characteristics [5].

The synergist has a structure capable of interacting with pigments and contains a functional group indicating high affinity with a dispersant, thus increasing the dispersion performance in

* Corresponding author.
E-mail address: jaepil@snu.ac.kr (J.P. Kim).

http://dx.doi.org/10.1016/j.jiec.2017.09.036
1226-086X/© 2017 The Korean Society of Industrial and Engineering Chemistry. Published by Elsevier B.V. All rights reserved.

the dispersion matrix [6]. Because chromatic features and transmittance are crucial to image quality, the spectral characteristics of the synergist must be contemplated for the ink of the color filter. Therefore, it is necessary to adopt a synergist, which has similar spectral characteristics to the pigment for the color filter.

Several studies have been carried out to introduce synergists to improve the dispersion of pigments applied to the color filter [5,7–9]. Those studies focused on a blue, a red, and a yellow pigment. To the best of our knowledge, the investigation of a new synergist for green pigments has not been reported. The present study was performed to propose new green synergists that can retain the color properties and increase the dispersion performance of a green pigment used in the color filter. Ultimately, the contrast ratio of the LCD color filter was enhanced by reducing the pigment particle size.

We synthesized synergists for enhancing the dispersion of pigment green 7, which is widely used as a green colorant for the color filter and exhibits inferior dispersion properties. The synergists are designed to ensure the color characteristics of the color filter by showing appropriate spectral characteristics for green. The phthalocyanine was modified to indicate a high intermolecular interaction between the synergist and the pigment. Furthermore, the bathochromic shift of the absorption wavelength was intended by chlorination, and various substituents were added as a dispersant-affinic group to interact with the dispersant: ester, carboxylic acid, primary amine, and tertiary amine. The dispersion characteristics and color properties were investigated by average particle size, polydispersed index (PDI), zeta potential, and UV–vis spectrometer. The interaction between the synergists and a dispersant was demonstrated by using FT-IR spectrometer. The contrast ratio of the green color filter with the pigment dispersion was then examined. Finally, a suitable synergist that can improve the dispersion of pigment green 7 was proposed. The results were used to increase the contrast ratio of a green color filter for LCDs.

Experimental

Materials

1,8-Diazabicyclo-7-undecene (DBU), 4,5-dichlorophthalonitrile, ethyl 4-hydroxy-3-methoxybenzoate, *N*, *N*-dimethyl-3-aminophenol, and 3-aminophenol were purchased from TCI, and $ZnCl_2$, potassium carbonate anhydrous, lithium hydroxide monohydrate, and 1-pentanol were purchased from Sigma-Aldrich. The other reagents and solvents were obtained from commercial suppliers. All chemicals were reagent-grade. Transparent glass substrates were provided by NTP, Inc., and acrylic polymer binder [9] was supplied by NDM, Inc.

Characterization and instruments

^{1}H NMR spectra were recorded on a Bruker Avance 500 spectrometer (National Center for Inter-University Research Facilities at Seoul National University) at 500 MHz using dimethyl sulfoxide-d6, chloroform-d with tetramethylsilane (TMS) Elemental analysis was performed with a Thermo Scientific Flash EA 1112 elemental analyzer. Matrix-Assisted Laser Desorption/Ionization-Time of Flight (MALDI-TOF) mass spectra were collected on a Voyager-DE STR Biospectrometry Workstation (National Center for Inter-University Research Facilities at Seoul National University). UV–vis absorption spectra were measured using a PerkinElmer Lambda 25 spectrophotometer, and Fourier transform infrared spectroscopy (FT-IR) was conducted using a Thermo Scientific Nicolet 6700. The particle size analysis was performed using a Photal Otsuka Electronics ELSZ-1000, samples were prepared by diluting the dispersion with PGMEA (0.1 wt.%). The thickness of the spin-coated color filter was measured using a KLA-TENCOR Nanospec AFT/200 alpha step. Transmission electron microscopy (TEM) was performed on an FEI Tecnai F20 with an acceleration voltage of 200 kV; samples were prepared according to the literature procedures [7]. Field-emission scanning electronic microscopy (FE-SEM) images were acquired on a Zeiss MERLIN Compact; Pt was coated on the samples using JEOL MSC-101 for 40 secs at a current strength of 40 mA to avoid charging of the surface. Atomic Force Microscopy (AFM) was undertaken using a Park Systems NX-10. The color properties and transmittance spectra of the color filters were measured on a Scinco color spectrophotometer. The contrast ratio were analyzed using Tsubosaka Electric CT-1 BSLE.

Synthesis

Synthesis of compound 1 (ethyl 4-(2-chloro-4,5-dicyanophenoxy)-3-methoxybenzoate)

4,5-Dichlorophthalonitrile (1 g, 5.10 mmol) and ethyl 4-hydroxy-3-methoxybenzoate (1.10 g, 5.61 mmol) were dissolved in dry DMF (50 mL) and anhydrous K_2CO_3 (3.52 g, 25.5 mmol) was added portion wise for 3 h. The mixture was stirred at 80 °C for 12 h under nitrogen atmosphere. The solution was then poured into ice water (100 mL) with vigorous stirring to precipitate the product. The resulting suspension filtered to give a white-yellowish powder. Pure product was collected by column chromatography on silica gel using MC/hexane (3:1) mixture as an eluent. Yield 66%; ^{1}H NMR ($CDCl_3$, 500 MHz, 25 °C, TMS): δ 7.87 (s, 1H, Ar-H), 7.77 (d, J = 10 Hz, 2H, Ar-H), 7.20 (d, J = 8.5 Hz, 1H, Ar-H), 6.88 (s, 1H, Ar-H), 4.43 (q, J = 7 Hz, 2H, ester-CH2), 3.85 (s, 3H, OCH3), 1.43 (t, J = 7.5 Hz, 3H, CH3); ^{13}C NMR ($CDCl_3$, 500 MHz, 25 °C, TMS): δ 165.36, 157.24, 150.71, 144.76, 135.41, 130.27, 128.83, 123.38, 122.13, 119.54, 115.35, 114.38, 114.28, 109.83, 61.54, 56.24, 14.32.

Synthesis of compound 2 (4-chloro-5-(3-(dimethylamino)phenoxy) benzene-1,2-dicarbonitrile)

The product was synthesized following the same procedure for ethyl 4-(2-chloro-4,5-dicyanophenoxy)-3-methoxybenzoate using 4,5-dichlorophthalonitrile (1 g, 5.10 mmol), 3-(dimethylamino) phenol (0.77 g, 5.61 mmol), DMF (50 mL), and anhydrous K_2CO_3 (3.52 g, 25.5 mmol). The crude product was purified by column chromatography on silica gel using EA/hexane (1:4) mixture as the eluent. Yield 73%; ^{1}H NMR (d6-DMSO, 500 MHz, 25 °C): δ 8.51 (s, 1H, Ar-H), 7.50 (s, 1H, Ar-H), 7.26 (t, J = 8.5 Hz, 1H, Ar-H), 6.64 (dd, J = 8.5, 2.5 Hz, 1H, Ar-H), 6.48 (t, J = 2.5 Hz, 1H, Ar-H), 6.36 (dd, J = 8.0, 2.5 Hz,1H, Ar-H), 2.91 (s, 6H, amine-CH3); ^{13}C NMR (d6-DMSO, 500 MHz, 25 °C): δ 157.07, 154.69, 152.25, 136.00, 130.66, 128.53, 121.93, 115.14, 114.98, 109.70, 109.16, 106.28, 103.27, 39.92.

Synthesis of compound 3 (4-(3-aminophenoxy)-5-chlorobenzene-1,2-dicarbonitrile)

The product was synthesized following the same procedure for ethyl 4-(2-chloro-4,5-dicyanophenoxy)-3-methoxybenzoate using 4,5-dichlorophthalonitrile (1 g, 5.10 mmol), 3-aminophenol (0.61 g, 5.61 mmol), DMF (50 mL), and anhydrous K_2CO_3 (3.52 g,25.5 mmol). The white yellowish solid was obtained that was purified by column chromatography on silica gel using MC/hexane (10:1) mixture as the eluent. Yield 78%; ^{1}H NMR (d6-DMSO, 500 MHz, 25 °C): δ 8.51 (s, 1H, Ar-H), 7.56 (s, 1H, Ar-H), 7.09 (t, J = 8 Hz, 1H, Ar-H), 6.49 (d, J = 8 Hz, 1H, Ar-H), 6.28 (t, J = 2.5 Hz, 1H, Ar-H), 6.23 (dd, J = 8, 2.5 Hz, 1H, Ar-H), 5.41 (s, 2H, amine-H); ^{13}C NMR (d6-DMSO, 500 MHz, 25 °C): δ 156.82, 154.85, 151.06, 136.08, 130.70, 128.91, 122.49, 115.14, 114.96, 111.38, 109.39, 105.92, 104.12.

Synthesis of compound GS-1 (2,9(10),16(17),23(24)-tetrachloro-3,9 (10),16(17),23(24)-tetra(4-(ethoxycarbonyl)-2-methoxyphenoxy) phthalocyaninatozinc (II))

A mixture of 4-(2-chloro-4,5-dicyanophenoxy)-3-methoxybenzoate (1.70 g, 4.80 mmol), $ZnCl_2$ (0.20 g, 1.44 mmol) and DBU (0.44 g, 2.88 mmol), in 1-pentanol (50 mL) was heated to 150 °C and stirred for 12 h under nitrogen atmosphere. The crude product was precipitated by pouring the reaction solution into methanol (100 mL). After filtering the mixture, the collected solid was dried under vacuum. The solid was loaded onto a silica gel column with a 10:1 mixture of methylene chloride/MeOH eluent. As the crude product elutes from the column, the green band was collected and dried to afford GS-1 as a green solid. Yield 78%; MALDI-TOF MS: m/z 1492.1 (100%, [M + H]). Elemental analysis: Calcd for $C_{72}H_{52}Cl_4N_8O_{16}Zn$: C, 57.95; H, 3.51; N, 7.51; O, 17.15. Found: C, 58.50; H, 3.55; N, 7.57; O, 17.28.

Synthesis of compound GS-2 (2,9(10),16(17),23(24)-tetrachloro-3,9 (10),16(17),23(24)-tetra(4-carboxy-2-methoxyphenoxy) phthalocyaninatozinc (II))

GS-2 was synthesized according to the literature procedures [10] using GS-1 (0.89 g, 0.59 mmol), $LiOH{\cdot}H_2O$ (1.57 g, 36.6 mmol) in 70% aqueous methanol (100 mL), and THF (30 mL). The product was dried under vacuum to give GS-2. Yield 79%; MALDI-TOF MS: m/z 1380.9 (100%, [M + H]). Elemental analysis: Calcd for $C_{64}H_{36}Cl_4N_8O_{16}Zn$: C, 55.69; H, 2.63; N, 8.12; O, 18.55. Found: C, 54.58; H, 2.66; N, 8.18; O, 18.84%.

Synthesis of compound GS-3 (2,9(10),16(17),23(24)-tetrachloro-3,9 (10),16(17),23(24)-tetra(3-(dimethylamino)phenoxy) phthalocyaninatozinc (II))

GS-3 was synthesized following the same procedure for GS-1 using 4-chloro-5-(3-(dimethylamino)phenoxy)benzene-1,2-dicarbonitrile (1.52 g, 5.10 mmol). ZnCl2 (0.21 g, 1.53 mmol) and DBU (0.47 g, 3.06 mmol), in 1-pentanol (50 mL). Column chromatography with an 80:1 mixture of chloroform/MeOH eluent was performed to obtain GS-3 as a green solid. Yield 71%; MALDI-TOF MS: m/z 1257.1 (100%, [M + H]). Elemental analysis: Calcd for $C_{64}H_{48}Cl_4N_{12}O_4Zn$: C, 61.19; H, 3.85; N, 13.38; O, 5.09. Found: C, 60.56; H, 3.90; N, 13.64; O, 5.19.

Synthesis of compound GS-4 (2,9(10),16(17),23(24)-tetrachloro-3,9 (10),16(17),23(24)-tetra(3-aminophenoxy)phthalocyaninatozinc (II))

The cyclotetramerization of 4-(3-aminophenoxy)-5-chlorobenzene-1,2-dicarbonitrile was carried out following the same procedure for GS-1 using 4-(3-aminophenoxy)-5-chlorobenzene-1,2-dicarbonitrile (1.38 g, 5.10 mmol), $ZnCl_2$ (0.21 g, 1.53 mmol) and DBU (0.47 g, 3.06 mmol), in 1-pentanol (50 mL). The reaction solution was dried at 80 °C under vacuum to remove 1-pentanol and DBU. The crude solid was dissolved in DMF and water was added dropwise to the solution with continuous stirring. The mixture solution was then cooled to 0–5 °C and kept 24 h to precipitate the product. The solid was then filtered out and dried under vacuum. The suspension of the product in MeOH was heated under reflux for 1 h to dissolve impurities. At the end of reflux, the mixture was cooled to room temperature. The green solid was collected by vacuum filtration and chromatographed on silica with THF as an eluent, followed by recrystallization in ethanol. Yield 46%; MALDI-TOF MS: m/z 1444.9 (100%, [M + H]). Elemental analysis: Calcd for $C_{56}H_{32}Cl_4N_{12}O_4Zn$: C, 58.79; H, 2.82; N, 14.69; O, 5.59. Found: C, 59.28; H, 2.79; N, 14.93; O, 5.70.

Preparation of pigment dispersion

Pigment green 7 was mixed with the prepared synergist, a dispersant polymer, and acrylic polymer binder in propylene glycol methyl ether acetate (PGMEA). Zr beads were then introduced into the mixture. After mixing, a pre-milling (60 min) was performed using a paint shaker, followed by main-milling (120 min) with 550 times/min. The pigment dispersion was isolated by vacuum filtering.

Preparation of color inks and spin-coated films

Pigment ink for a color filter was comprised of PGMEA (2.10 g), acrylic polymer binder (2.74 g), pigment dispersion (0.15 g). The acrylic polymer binder (Mw 16,000 g/mol) [9] was dissolved in PGMEA, followed by adding pigment dispersion, and then the mixture was stirred vigorously for 120 min at room temperature. The prepared inks were coated on a transparent glass substrate using a MIDAS System SPIN-1200D spin coater. The ink-coated glasses were then pre-baked at 100 °C for 100 secs and post-baked at 230 °C for 30 min. After post-baking, the coordinate values of the pigment-coated glasses were measured.

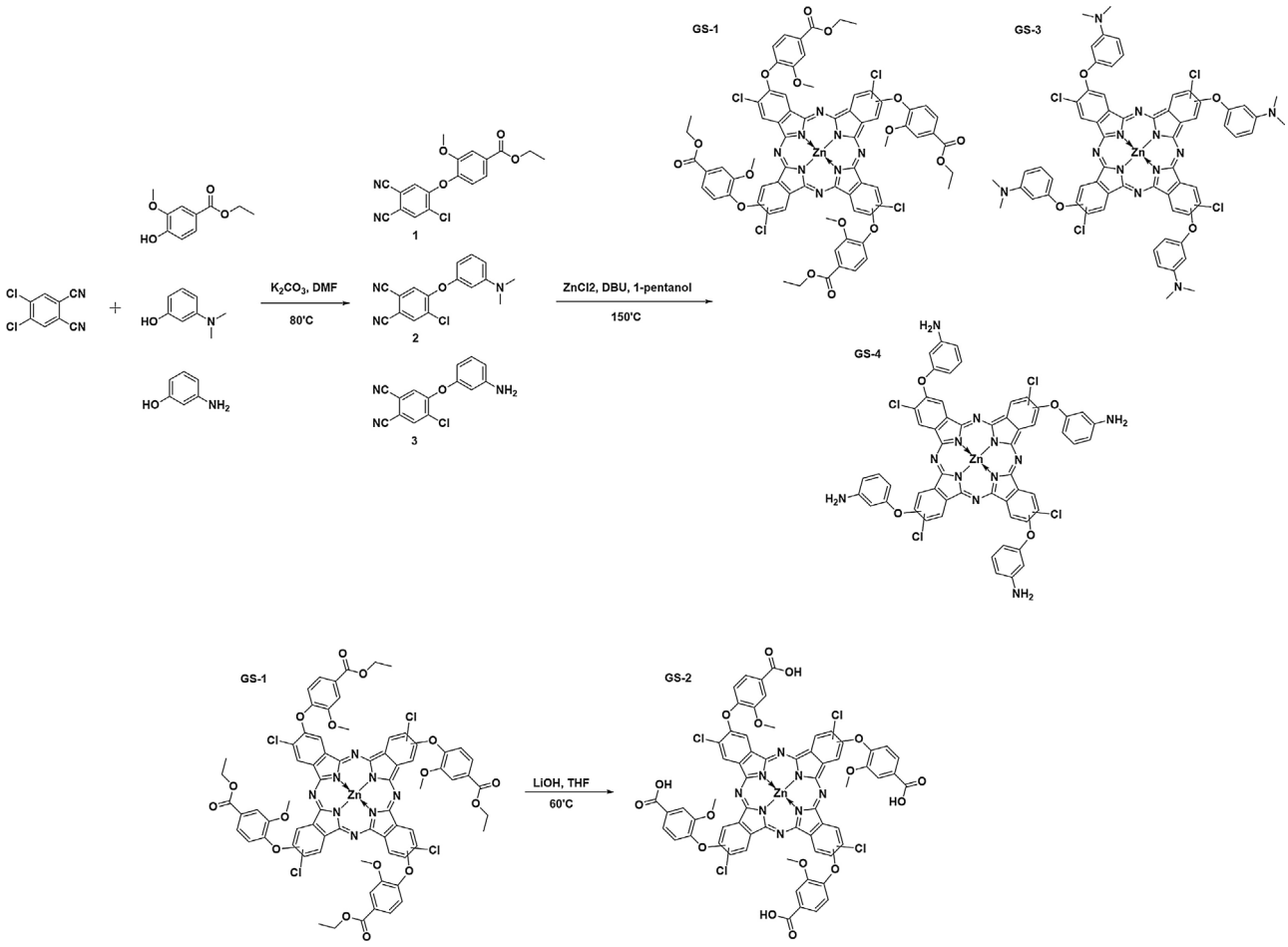
Results and discussion

Design and synthesis of the synergists

A synergist should interact intimately with the target pigment to function effectively in the dispersion process, and this can be mediated by different types of forces like ionic, hydrogen-bonding, and van der Waals interactions [4]. For phthalocyanine, two parts, *viz.*, the hydrophilic metal cation in the center of the macrocycle and the hydrophobic isoindole rings at the periphery of the macrocycle [11], could be used to react with the synergist. However, the phthalocyanine-based pigment, like pigment green 7, has a strong tendency to aggregate because of its planar structure, and this attractive interaction hinders the reaction between both these sites and the synergist [4]. Therefore, large planar structures could be effective for adsorbing on such aromatic macrocyclic compounds. Therefore, we employed phthalocyanine moieties and induced the π-π stacking interaction that readily occurs between large planar molecules. The functional groups (ester, carboxylic acid, tertiary amine, and primary amine) were adopted for the phthalocyanine derivatives to interact with pigment-affinic groups of a dispersant such as aminic and carbonyl groups. In addition, chlorine and phenoxy groups, which are electron-donating groups, were introduced at the peripheral position of the phthalocyanine to provoke the bathochromic shift of the Q-band, causing spectral characteristics corresponding to green [12].

The phenyl derivatives with each functional group were substituted by one equivalent of 4,5-dichloro phthalonitrile through the SN reaction. The zinc(II) phthalocyanine was then prepared by cyclotetramerization of the phthalonitriles with zinc chloride. This is displayed in Scheme 1. The synthesis of the precursors was carried out using DMF as a solvent and a base of K_2CO_3. 1-Pentanol, and DBU was used as a nucleophile and a non-nucleophilic base catalyst for the cyclotetramerization of the phthalonitriles [12].

The synthesized phthalonitriles and phthalocyanines were purified by column chromatography. GS-4 was further purified by recrystallization using ethanol. Theoretically, all synergists can have constitutional isomers. Because the isomers hardly influence the dispersion of the pigment, the test in this study was conducted without separation of the isomers. The prepared materials were obtained with a yield of 30–80% depending on the substituent. Their structure was confirmed by NMR, MALDI-TOF-MS, and the elemental analyzer.



Scheme 1. Synthetic route of the prepared synergists.

Spectral properties of the synergists

The prepared synergists should transmit the region of 500–550 nm for the green color filter. To confirm the absorption and transmission of the synergists, the optical properties were evaluated by UV–vis spectroscopy. The results are shown in Fig. 1.

The phthalocyanine structurally forms the heteroaromatic 18–π electron system of 16–membered ring, and that π-electron rich system leads to π–π* transition. This electronic transition is the origin of absorption spectra of phthalocyanine analogues. They typically present the Q-band (600–700 nm) and B-band (300–400 nm) absorption spectra. The absorption of Q-band is attributed to the electronic transition from HOMO of π-bond to LUMO of that bond, and B-band is attributed to the electronic transition from deeper HOMO to LUMO [13].

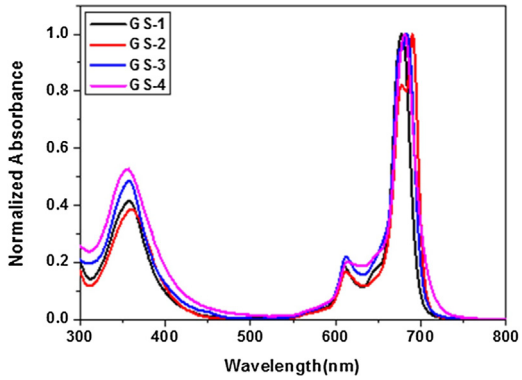


Fig. 1. Normalized absorption spectra of the synthesized synergists in PGMEA.

GS-1, GS-2, GS-3, and GS-4 exhibited maximum absorption at 678 nm, 690 nm, 684 nm, and 681 nm, respectively, and transmitted light in 500–550 nm region, which is required for the green color filter. Q-band of unsubstituted zinc phthalocyanine is generally shown (or displayced) near 650 nm. On the other hand, all synthesized dye indicated bathochromically shifted Q-band, compared to unsubstituted zinc phthalocyanine. This red shift of Q-band is due to a substitution of electron donating groups on the phthalocyanine. As the electron donating substituents, such as hydroxy-, alkoxy-, and aryloxy groups, were substituted on peripheral or non-peripheral positions of phthalocyanine, the electron density of isoindole rings of phthalocyanine is increased. This enhancing of electron density on phthalocyanine core leads to a shift of the first oxidation and first reduction potential, thus decreasing the HOMO-LUMO gap. As a result, the Q-band also moves to a longer wavelength [14].

The maximum absorption wavelength of GS-2 was slightly longer than that of GS-1, and the Q-band was weakly split, unlike other synergists. This difference is due to the D_2h symmetry characteristic [15], which is enhanced by the solvation of the carboxylic acid in the DMF of a polar solvent [16]. All other synergists indicated a similar maximum absorption characteristic of approximately 680 nm.

Although GS-2 showed a weakly split Q-band, this phenomenon had little effect on its transmission wavelength range. Thereby, all

synthesized synergists transmitted green light range (500–550 nm) for use in the color filter.

Dispersion capability of the synergists

The pigment was mixed with the prepared synergists, the dispersant, and Zr-bead in PGMEA. The mixture was then dispersed by using a paint shaker [17]. To confirm the dispersion performance, the particle size was measured by DLS.

As shown in Table 1, the average particle sizes of the pigment with GS-1 and GS-3 were 119.9 nm and 123.9 nm, respectively, those of GS-2 and GS-4 were 94.3 nm and 98.9 nm, respectively, and that without a synergist was 118.6 nm. These results indicate that GS-1 and GS-3 containing ester and tertiary amine were ineffective for reducing the particle size compared with the non-synergist pigment dispersant. In contrast, GS-2 and GS-4 with carboxylic acid and primary amine displayed considerably decreased particle size, indicating that those molecules are suitable as the synergist.

In GS-1 and GS-3, ethyl and methyl groups are introduced at carboxylate and amine groups, respectively, whereas hydrogen, not an alkyl group, is substituted in the cases of GS-2 and GS-4. Thus, it is assumed that because the terminal alkyl groups of ester and tertiary amine induce steric hindrance and interfere with the interaction between the pigment-affinic group of the dispersant and carboxylate and amine of GS-1 and GS-3, the dispersion was not performed properly. On the contrary, GS-2 and GS-4 contain carboxylic acid and primary amine, which have hydrogen readily capable of hydrogen bond formation. Thus, it is inferred that an interaction such that hydrogen bonds between the dispersant and synergist could be provoked by an elimination of the steric hindrance, thereby reducing the particle size.

The polydispersity index (PDI) of all the dispersed particles was measured to be 0.1–0.2, which indicates that the size distribution of the particles in the dispersion is narrow. Moreover, the result is consistent with that of the average particle size. GS-2 and GS-4 displayed smaller values of PDI among the different dispersions. This fact confirms that these synergists are efficient in improving the dispersity of the pigment particles.

The state of the pigment dispersion was also observed using TEM micrographs, indicated in Fig. 2. The dispersed pigment nanoparticles without a synergist exhibited a large particle size and agglomerated together forming clusters. The similar phenomenon was shown in the dispersion with GS-1 or GS-3, which were not effective in reducing particle size. In contrast, ones with GS-2 or GS-4 as a synergist displayed uniformly dispersed state. Thus, this result suggests that those pigment dispersions of the former have not only a large particle size but also a low uniformity. However, the size of agglomerates of those is smaller than that of the dispersion which does not use a synergist. Therefore, it is also inferred through the TEM images that the synergists can inhibit the agglomeration by being present between pigment particles.

In the dispersion of pigments, the dispersion stability is also important. When the dispersion is labile, the particle can grow by agglomeration [18], thereby changing the color characteristic. For this, we analyzed the zeta potential of the pigment dispersions to investigate their stability. Moreover, the particle size of the dispersions was evaluated after ten weeks. The results are provided in Table 1. The zeta potential increased from −11 mV for dispersions with no synergist to +14 and +8 mV for dispersions with GS-2 and GS-4, respectively. However, dispersions with GS-1 and GS-3 showed no significant change with an increase in the zeta potential values to 5–6 mV. The adsorption on the pigment surface *via* amine anchoring groups of the dispersant shifts the surface potential in the positive direction [19]. Thus, the improvement in the zeta potential implies that the surface of the pigment particles is increasingly covered with the dispersing agent, and this leads to the separation of the particles *via* steric stabilization of the polymeric dispersant. Thus, GS-2 and GS-4 enhance the degree of the surface adsorption of the dispersant, and act as a bridging agent between the pigment and dispersant.

On the contrary, in terms of the long-term stability after storage for ten weeks, dispersions with GS-2 exhibit superior stability, showing the growth of the particle by 8.1 nm, and those with GS-1, GS-3, and GS-4 showed a similar growth with an increase in the particle size by 12.6, 13.4, and 13.9, respectively. This is presumably due to the stronger electrostatic interaction between the carboxylic acid and amine groups. It is accepted that the carboxylic acid group is one of the excellent hydrogen-bond donors and acceptors. Thus, comparing GS-2 with GS-4, it can be concluded that a combination of the carboxylic acid/amine anchoring group is better than that of the amine/amine anchoring group, inducing stronger intermolecular interaction with the dispersant. This excellent hydrogen bonding ability leads to a better stability of the pigment dispersion with GS-2 tohan that with GS-4.

Furthermore, it is clear that the particle size growth of the pigment dispersions with synergists was smaller than that of the dispersion without a synergist. This difference means that the synergists exist between the pigment particles and suppress an aggregation of the particles by steric hindrance of those bulky substituents, they were adsorbed on the pigment as intended. Accordingly, the introduction of the prepared synergists can be effective for enhancing the stability.

Among the synergists, GS-2 showed outstanding dispersion performance in both particle size and stability, and GS-4 also displayed similar capability in reducing the particle size. These results obtained in the pigment dispersion properties indicate that functional groups such as carboxylic acid and primary amine, which can induce electrostatic attraction such as hydrogen bonding [20,21], can improve the dispersion of pigment green 7. Furthermore, an introduction of all prepared synergists can improve the dispersion stability, compared to the non-synergist dispersion.

Table 1
Average particle size, PDI, and zeta potential of dispersed pigment pastes in PGMEA (0.1 wt%). The samples were stored at room temperature for ten weeks and then analyzed by the same method.

Pigment	Synergist	Average Particle size (nm)	PDI	Zeta potential (mV)	Average Particle size (nm) (after 10 weeks)	Δ (nm)
Pigment green 7	No synergist	118.6	0.174	−11	156.5	37.9
	GS-1	119.9	0.182	−5	132.5	12.6
	GS-2	94.3	0.112	+14	102.4	8.1
	GS-3	123.9	0.177	−7	137.3	13.4
	GS-4	98.9	0.113	+8	112.8	13.9

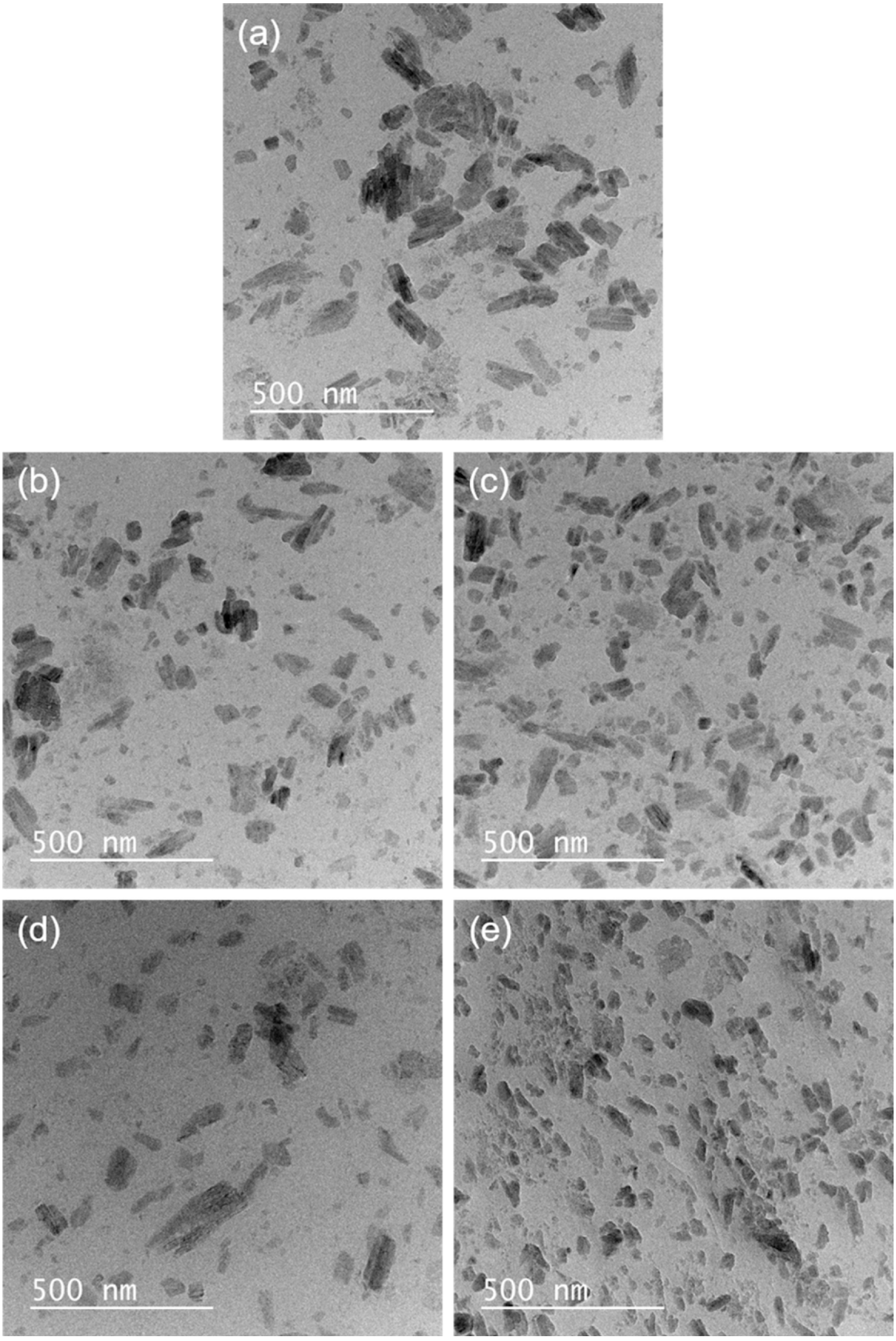


Fig. 2. Transmission electron microscopy images of dispersed pigment nanoparticles coated on ultrathin amorphous carbon film: (a) pigment G7 without synergist, (b) with GS-1, (c) with GS-2, (d) with GS-3, (e) with GS-4.

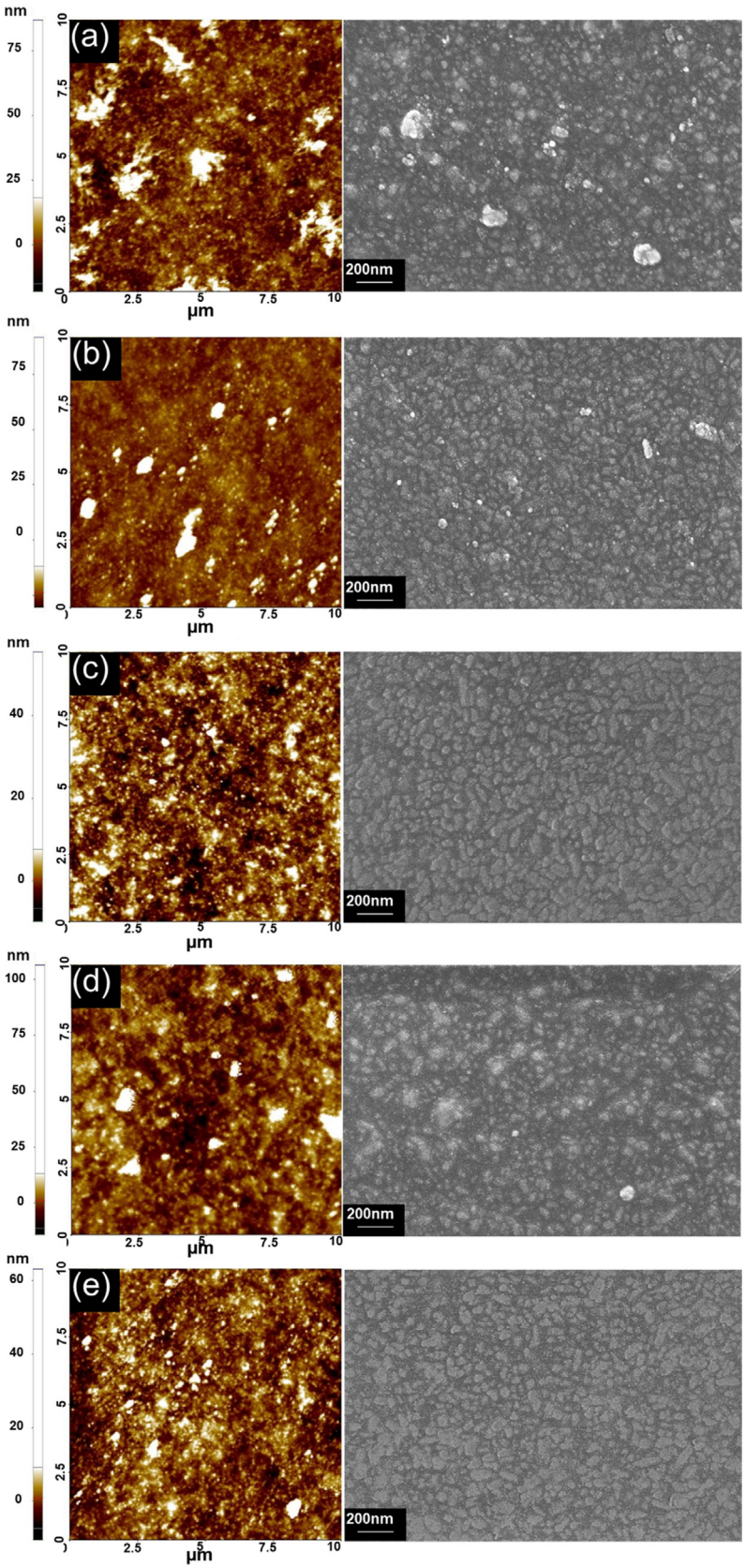


Fig. 3. Atomic force microscopy images ($10 \times 10\ \mu m^2$) (left) and scanning electron microscopy (right) images of pigment nanoparticles dispersions spin-coated on glass: (a) pigment G7 without synergist, (b) with GS-1, (c) with GS-2, (d) with GS-3, (e) with GS-4.

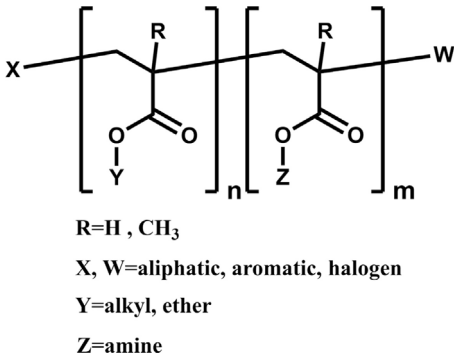


Fig. 4. The common structure of acrylic block copolymer dispersants.

However, because all pigment dispersions tend to increase in particle size over time, further studies are needed to address this issue.

AFM and SEM analysis of spin-coated pigment nanoparticle dispersions

The surface of spin-coated films on glass was analyzed by using AFM and SEM, to observe coatings of pigment nanoparticle dispersions.

As displayed in Fig. 3, the pigment nanoparticle film without a synergist showed a rough surface with various clusters of agglomerates having a height of 50–100 nm. It appears that those clusters were caused by particles which were not properly dispersed. This result corresponds well with those found in the TEM analysis above. Because the dispersion is not uniform, particles having different sizes are present in an unstable state. Therefore, those particles can easily flocculate in the film [22,23], and large particles can stick out of the coating. Those phenomena resulted in the surface irregularity of the film. A similar result was also exhibited in pigment dispersions using GS-1 or GS-3. Various agglomerates were observed on the surface of each film using those synergists. However, those films with GS-1 or GS-3 showed smaller agglomerates and clusters, compared with pigment dispersion film containing no synergist. As stated above, this result demonstrates that the synergists can inhibit a formation of large clusters of agglomerates on the surface of a coating.

Meanwhile, in the case of films with thoroughly dispersed pigments using GS-2 or GS-4, the coatings displayed few and small agglomerates and had a clearer surface than those of the dispersions with no synergist, GS-1, or GS-3. This phenomenon implies that their excellent dispersion state obtained by a suitable synergist can be efficiently retained in their coatings.

The surface analysis micrographs of the pigment dispersion coatings by AFM and SEM showed the similar tendency with those of TEM. The result revealed that all dispersions using synergists had a smaller size of agglomerates and the dispersion of GS-2 or GS-4 particularly displayed minimal agglomeration. Hence, the synergists can not only enhance the stability of dispersion particles in a liquid state but also help to sustain that in the coating.

FT-IR spectra of the synergists and dispersant blend

A polymeric dispersant is commonly used to disperse phthalocyanine derivatives such as pigment green 7, and an acrylic block copolymer dispersant with an amine value of 40 mg (KOH/g) was adopted in this study. The structure of a typical acrylic block copolymer dispersant is mainly composed of two parts [24,25] as shown in Fig. 4. The anchoring block of a polymeric dispersant for organic pigments mainly incorporates an aminic group, because that functional group is effective in diverse pigments [26]; various aminic groups are introduced in dispersants.

As stated above, GS-2 and GS-4, which contain carboxylic acid and primary amine, respectively, reduce the particle size of the pigment. Those functional groups have hydrogen combined with a highly electronegative atom such as oxygen and nitrogen; this circumstance can provide a proper condition for hydrogen bonds with the dispersant. Thus, it is inferred that GS-2 and GS-4 present superior dispersion properties unlike GS-1 and GS-3. Eventually, it is considered that the hydrogen bonds are provoked between those carboxylic acid and primary amine group of the synergists and the aminic group of the anchoring block in the dispersant. This interaction is briefly illustrated in Fig. 5. We used FT-IR

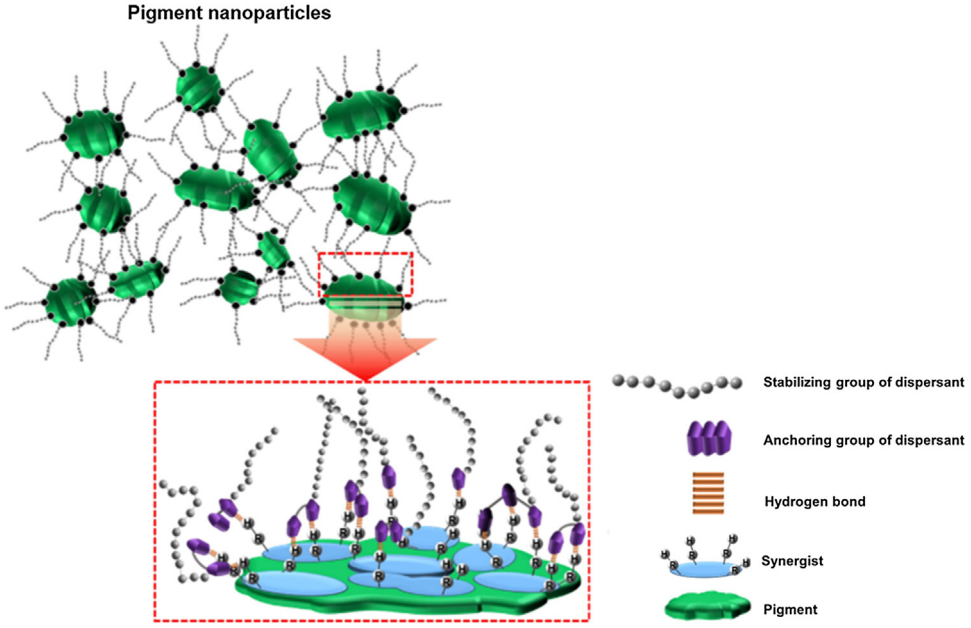


Fig. 5. Interaction of synergists with polymeric dispersants.

spectroscopy to identify the hydrogen bonds between the dispersant and the synthesized synergists. Films without dispersant were also prepared for comparison; the IR spectra obtained from the samples are presented in Fig. 6.

In GS-1 and GS-3, the spectra showed no significant difference between the film with dispersant and that without dispersant. In the case of GS-1 without the dispersant, a strong C=O stretching band for ester near 1713 cm^{-1} appeared, and no specific absorption band of hydrogen bonding O—H was found [27]. A similar tendency was observed when dispersants were mixed with GS-1. GS-3, which is substituted the tertiary amine, also showed no absorption band for hydrogen bonding in the range of 3100–3500 cm^{-1}. For the mixture of GS-3 and the dispersant, that indicated no significant change of absorption band, identically to GS-1.

However, the results of GS-2 and GS-4 displayed a different propensity. The spectrum of GS-2 exhibited a broad hydrogen bonding O—H band in the range of 2700–3400 cm^{-1}; this was the result of the formation of strong self-associated hydrogen bonding between the carboxylic acids of GS-2 molecules [27]. Moreover, it should be noted that additional broad peaks were observed near 1640 cm^{-1} apart from a strong aryl conjugated C=O band at 1686 cm^{-1}. This was presumably due to the hydrogen-bonded C=O band [27,28]. Thus, the C=O stretching band can be found in company with the free C=O band at a lower wavenumber. On the contrary, in the result of GS-2 mixed with dispersant, the hydrogen-bonded C=O band near 1640 cm^{-1} was hardly observed, and the width of the strong aryl conjugated C=O band was narrowed. This is the result of a decrease in the self-associated hydrogen bonds of the C=O group. It is inferred that the anchoring group of the dispersant and the O—H in the carboxylic acid of GS-2 were interassociated with each other, forming a hydrogen bond, and this interaction suppressed the self-associated hydrogen bond of the carboxylic acid [29]. In addition, for the non-dispersant sample of GS-2, the higher absorption peak of the self-associated O—H stretching band appeared at 2925 cm^{-1}, while that peak of the dispersant mixture moved to a 76 cm^{-1} higher frequency of 3001 cm^{-1}. It seems that the self-associated hydrogen bond of GS-2 decreased and the stretching band shifted slightly to a higher wavenumber, owing to the formation of hydrogen bond between GS-2 and the dispersant [29–31]. Therefore, these results support the formation of a hydrogen bond between GS-2 and the dispersant effectively, as suggested.

Doublet peaks were found in the range of 3386 cm^{-1} and 3477 cm^{-1}. The typical N—H stretching band for primary amine, and the N—H bending band was observed at 1535–1648 cm^{-1} in the GS-4 without the dispersant [27]. However, the GS-4 film containing the dispersant showed that those peaks at 3296 cm^{-1} and 3385 cm^{-1} broadened and moved to approximately 90 cm^{-1} lower frequency. These changes appear to be caused by the formation of the hydrogen bonding between a dispersant and primary amine of GS-4 [32]. The hydrogen bond of amines theoretically generates shifting of the N—H stretching band to a lower wavenumber and broadening of the band. Consequently, these results suggest that GS-4 is also interassociated with the dispersant, forming a hydrogen bond.

As a result of FT-IR measurement, we confirm that GS-2 and GS-4 could form a hydrogen bond with the dispersant, as predicted. It

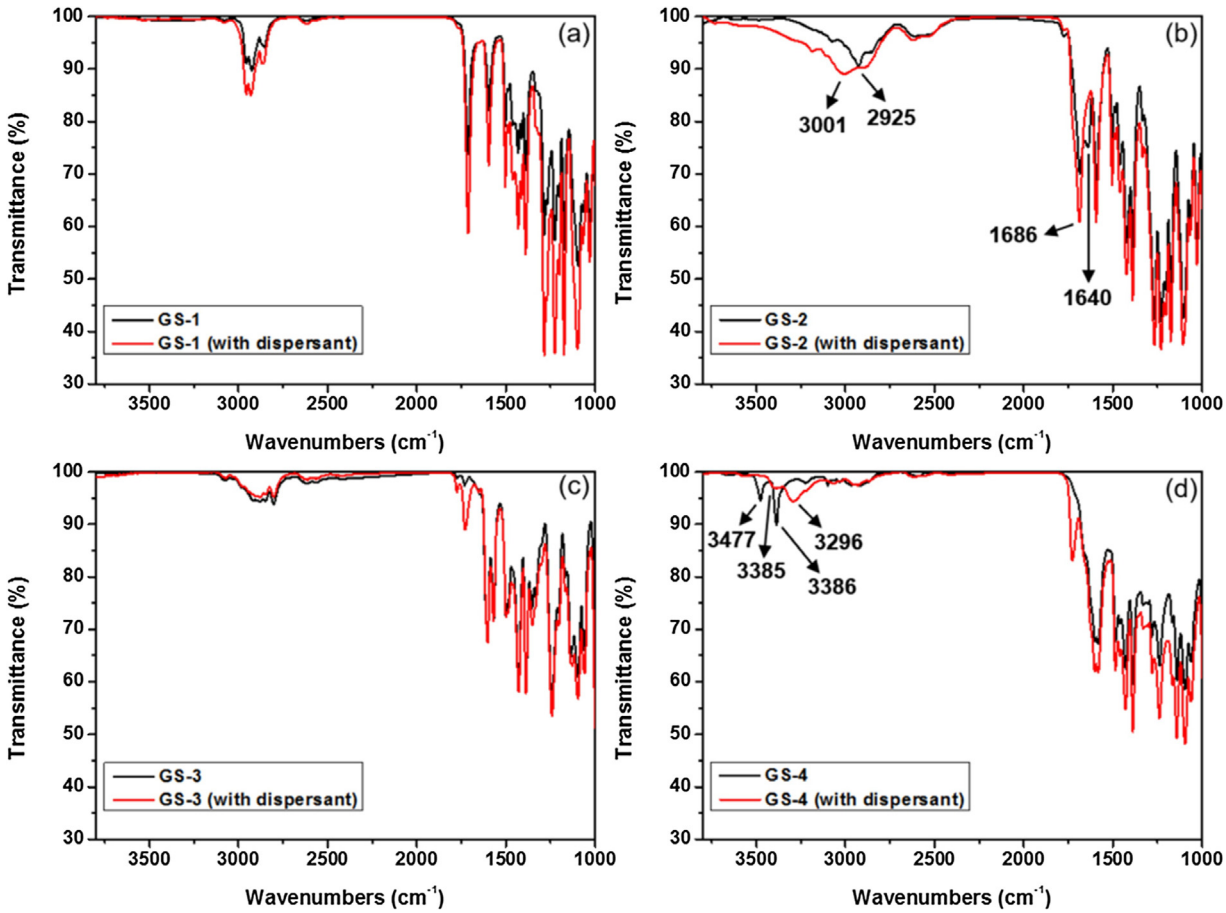


Fig. 6. FT-IR spectra of the synergist and the dispersant blended films. The synergist and the dispersant mixtures in PGMEA were spin-coated on glass and then analyzed: (a) GS-1, (b) GS-2, (c) GS-3, (d) GS-4.

Table 2
Maximum and minimum brightness (Y) and a contrast ratio of the color filter with pigment pastes. The pigment inks were spin-coated on glass, followed by baking at 230 °C.

Pigment	Synergist	Y_{max}	Y_{min}	CR	Thickness
Pigment green 7	No synergist	837.6	0.171	4885	2.56
	GS-1	826.7	0.169	4904	2.60
	GS-2	843.6	0.149	5646	2.39
	GS-3	834.8	0.170	4923	2.45
	GS-4	825.1	0.150	5518	2.36

is postulated that GS-2 and GS-4 showed superior dispersion performance than GS-1 and GS-3 owing to those interassociations with the dispersant.

Contrast ratios of spin-coated color filters

The contrast ratio of the LCD is closely related to the particle size of the pigment applied to the color filter [1,9]. When the particle size of the pigment is large, the light from the backlight unit is scattered, and the polarization is altered; thus, uncontrolled light is transmitted, and the contrast ratio is reduced [33]. To demonstrate whether the particle size reduced by the synergist can enhance the contrast ratio, we fabricated color filters using dispersed pigment pastes with the synergists and measured their features. This is shown in Table 2.

The contrast ratio is determined as the ratio of the maximum brightness to the minimum brightness (Y_{max}/Y_{min}). Thus, it is necessary to increase the maximum brightness or decrease the minimum brightness to improve the contrast ratio. The maximum brightness is influenced by the light source and can be easily enhanced by changing the type or voltage of the light source. In contrast, the minimum brightness is concerned with the material used in the color filter because the scattering occurs as the light passes through the color filter, and the light leaks out of a polarizer film, as described above. Accordingly, reducing the minimum brightness is a key point to improve the contrast ratio of the LCD.

Table 2 shows that the contrast ratio of ref., GS-1, GS-2, GS-3, and GS-4 are 4885, 4904, 5646, 4923, and 5518, respectively, and the pigment pastes with GS-2 and GS-4 indicated higher values than the others. This is similar to the particle size measurement result above, meaning that a reduction in particle size by the synergists helps increase the contrast ratio value. This can be clearly confirmed from the minimum brightness value. No-synergist, GS-1, GS-2, GS-3, and GS-4 displayed the Y_{min} values of 0.171, 0.169, 0.149, 0.170, and 0.150, respectively. GS-2 and GS-4 with reduced particle size exhibited reduced values 15% and 14% lower than that of ref., respectively, whereas the variations of maximum brightness values are less than 3%. It is inferred that as the particle size of the pigment dispersion decreases, the scattering of light is reduced, and the leakage of light is suppressed. Hence, the maximum brightness value was similar, but the minimum brightness value was decreased, and the contrast ratio was improved by more than 13% compared to that of the non-synergist, GS-1, and GS-3.

In conclusion, it is confirmed that the prepared synergists of GS-2 and GS-4 reduce the minimum brightness value by decreasing the particle size of the pigment dispersion, and those synergists are effective for improving the contrast ratio.

Table 4
The coordinate values corresponding to the CIE 1931 chromaticity of the color filters with pigment pastes.

Pigment	Synergist	x	y	Y
Pigment green 7	No synergist	0.1552	0.4160	34.99
	GS-1	0.1556	0.4160	34.79
	GS-2	0.1581	0.4160	35.73
	GS-3	0.1567	0.4160	34.75
	GS-4	0.1592	0.4160	35.33

Spectral and chromatic properties of spin-coated color filters

Finally, the spectral and color characteristics of the spin-coated color filter with the prepared pigment dispersion were measured by using UV–vis spectrometry and color spectrometry; Tables 3 and 4 and Fig. 7 indicate each property. The color coordinate values were compared based on the same y value to evaluate the differences precisely.

It is observed that all measured color properties displayed similar x values. This means that the synthesized synergists rarely influence the color of the pigment dispersion and have appropriate color characteristics for use in the green color filter. In the case of brightness (Y), GS-2 and GS-4 with superior dispersion characteristics exhibited slightly higher values than those of no synergist, GS-1, and GS-3. This difference is presumed to result from the smaller particle size of the pigment dispersion. This hypothesis can be confirmed from the transmission spectra: GS-2 and GS-4 also showed slightly higher transmittance in the range of 500–505 nm of the maximum transmission region. Thus, the difference in the transmission of the GS-2 and GS-4 appears to be reflected by the higher brightness.

It is observed that all measured color properties displayed similar x values. This means that the synthesized synergists rarely influence the color of the pigment dispersion and have appropriate color characteristics for use in the green color filter. In the case of brightness (Y), GS-2 and GS-4 with superior dispersion characteristics exhibited slightly higher values than those of no synergist, GS-1, and GS-3. This difference is presumed to result from the smaller particle size of the pigment dispersion. This hypothesis can be confirmed from the transmission spectra; GS-2 and GS-4 also showed slightly higher transmittance in the range of 500–505 nm of the maximum transmission region. Thus, the difference in the transmission of the GS-2 and GS-4 appears to be reflected by the higher brightness.

The results of spectral and color characteristics demonstrate that the chromatic features of all prepared color filters were similar to that of the non-synergist color filter, and the synergists have a suitable spectral property as a colorant for the green color filter.

Conclusions

Four phthalocyanine-based synergists were synthesized and introduced to improve the dispersion properties of pigment green

Table 3
The transmittance of the color filters with pigment pastes.

Pigment	Synergist	Trasmittance (at 500 nm)	Trasmittance (at 505 nm)
Pigment green 7	No synergist	79.5	79.6%
	GS-1	79.4	78.8
	GS-2	80.4	80.0
	GS-3	79.0	78.7
	GS-4	80.4	79.6

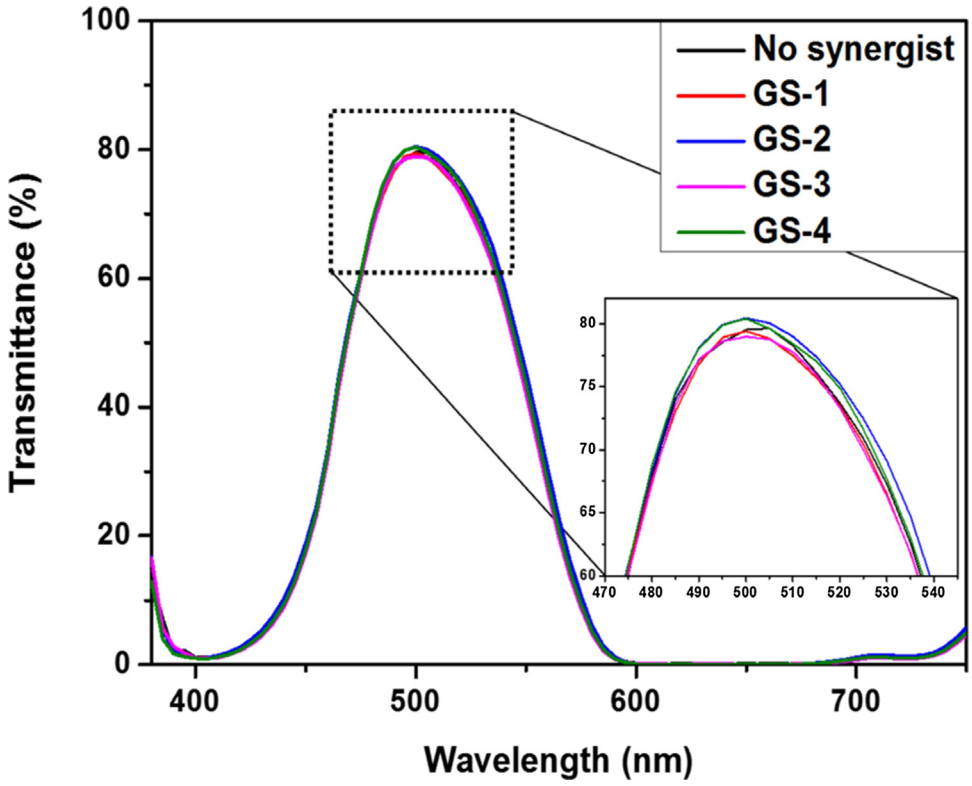


Fig. 7. Transmittance spectra of the color filter with pigment pastes. The maximum transmittance (dashed rectangular box) was shown in an enlarged scale.

7 and increase the contrast ratio of the color filter. All the synergists showed suitable absorption bands, transmitting in the green wavelength region (500–550 nm). GS-2 and GS-4 decreased the particle size of the pigment, thereby indicating that the carboxylic acid and primary amine groups are effective in improving the dispersion characteristics. These functional groups can form strong hydrogen bonds with the anchoring group of the dispersant. In addition, the result of PDI confirms the stabilization of the pigment by these synergists. The zeta potential values indicated good degree of the surface coverage due to the strong electrostatic interaction between the synergists and the dispersant. It is concluded that the synergists adsorb appropriately on the pigment surface and act as a bridge between the pigment and dispersing agent. The SEM and TEM images suggested a thoroughly dispersed state of the particles. The FT-IR spectra demonstrated hydrogen bonding between GS-2 or GS-4 and the dispersant, confirming the interaction between the synergist and the dispersant. Finally, it is ascertained that the pigment pastes with reduced particle sizes obtained by the use of GS-2 and GS-4 could improve the contrast ratio of the color filter without any migration of the color property.

In conclusion, we have suggested a suitable molecule structure as the synergist for dispersing phthalocyanine-based pigment used in the green color filter. However, regardless of the synergists existence, the dispersed pigment pastes were found to agglomerate over time. This issue is one of the disadvantages of the pigment dispersion method. Thus, further studies will be needed to suppress the agglomeration or introduce another color filter method that does not require the dispersion process such as a dye-based color filter.

Acknowledgements

This work was supported by LG Display Ltd and Research Institute of Advanced Materials (RIAM).

Appendix A. Supplementary data

Supplementary data associated with this article can be found, in the online version, at http://dx.doi.org/10.1016/j.jiec.2017.09.036.

References

[1] C.G. Jhun, J.S. Gwag, J. Opt. Soc. Korea 18 (2014) 184.
[2] B.J. Berne, R. Pecora, Dynamic Light Scattering: With Applications to Chemistry, Biology, and Physics, (2013) .
[3] P. Piedra, H. Moosmüller, Sol. Energy 155 (2017) 637.
[4] F.O. Pirrung, P.H. Quednau, C. Auschra, CHIMIA Int. J. Chem. 56 (2002) 170.
[5] M.M. Gacek, J.C. Berg, Electrophoresis 35 (2014) 1766.
[6] J.J. Florio, D.J. Miller, Handbook of Coating Additives, Taylor & Francis, 2004.
[7] A.T. Kelley, P.J. Alessi, J.E. Fornalik, J.R. Minter, P.G. Bessey, J.C. Garno, T.L. Royster, ACS Appl. Mater. Interfaces 2 (2010) 61.
[8] C. Yoon, J.-H. Choi, J.P. Kim, Mol. Cryst. Liq. Cryst. 533 (2010) 102.
[9] C. Yoon, J.-h. Choi, Dyes Pigm. 101 (2014) 344.
[10] V.T. Verdree, S. Pakhomov, G. Su, M.W. Allen, A.C. Countryman, R.P. Hammer, S. A. Soper, J. Fluoresc. 17 (2007) 547.
[11] K. Kadish, R. Guilard, K.M. Smith, The Porphyrin Handbook: Phthalocyanines: Properties and Materials, Elsevier, 2012.
[12] V.N. Nemykin, E.A. Lukyanets, Arkivoc (2010) 136.
[13] K.J. Hamam, M.I. Alomari, Appl. Nanosci. 7 (2017) 261.
[14] V.N. Nemykin, E.A. Lukyanets, ARKIVOC (2010) 136.
[15] J. Mack, N. Kobayashi, Chem. Rev. 111 (2011) 281–321.
[16] S. Gaspard, T.-H. Tran-Thi, J. Chem. Soc. Perkin Trans. 2 (1989) 383.
[17] W. Herbst, K. Hunger, Industrial Organic Pigments: Production, Properties, Applications, Wiley, 2006.
[18] H.J. Spinelli, Adv. Mater. 10 (1998) 1215.
[19] F. Babick, Suspensions of Colloidal Particles and Aggregates, Springer International Publishing, 2016.
[20] S. Creutz, R. Jerome, Langmuir 15 (1999) 7145.
[21] J.R.C. Costa, C. Correia, J.R. Góis, S.M.C. Silva, F.E. Antunes, J. Moniz, A.C. Serra, J. F.J. Coelho, Prog. Org. Coat. 104 (2017) 34.
[22] L.S. Kotlyar, B.D. Sparks, Y. Lepage, J.R. Woods, Clay Miner. 33 (1998) 103.
[23] F. Müller, W. Peukert, R. Polke, F. Stenger, Int. J. Miner. Process. 74 (2004) S31.
[24] P.T. Lee, C.W. Chiu, L.Y. Chang, P.Y. Chou, T.M. Lee, T.Y. Chang, M.T. Wu, W.Y. Cheng, S.W. Kuo, J.J. Lin, ACS Appl. Mater. Interfaces 6 (2014) 14345.
[25] S. Creutz, R. Jérôme, G.M.P. Kaptijn, A.W. Werf, J.M. Akkerman, J. Coat. Technol. 70 (1998) 41.
[26] C. Auschra, E. Eckstein, A. Mühlebach, M.-O. Zink, F. Rime, Prog. Org. Coat. 45 (2002) 83.

[27] D.L. Pavia, G.M. Lampman, G.S. Kriz, J.A. Vyvyan, Introduction to Spectroscopy, Cengage Learning, 2014.
[28] L. Guo, H. Sato, T. Hashimoto, Y. Ozaki, Macromolecules 43 (2010) 3897.
[29] N.-X. Chen, J.-h. Zhang, Chin. J. Polym. Sci. 28 (2010) 903.
[30] S. Thayumanasundaram, V.S. Rangasamy, N. De Greef, J.W. Seo, J.-P. Locquet, Eur. J. Inorg. Chem. (2015) 1290.
[31] M.M. Coleman, D.J. Skrovanek, J. Hu, P.C. Painter, Macromolecules 21 (1988) 59.
[32] L.-S. Teo, C.-Y. Chen, J.-F. Kuo, Macromolecules 30 (1997) 1793.
[33] M. Yoneya, Y. Utsumi, Y. Umeda, J. Appl. Phys. 98 (2005) 016106.